Toughness scale from first principles

Shigenobu Ogata[1] and Ju Li[2,a)]
[1]*Department of Mechanical Science and Bioengineering, Graduate School of Engineering Science, Osaka University, Osaka 560-8531, Japan*
[2]*Department of Materials Science and Engineering, University of Pennsylvania, Philadelphia, Pennsylvania 19104-6272, USA*

(Received 26 May 2009; accepted 31 October 2009; published online 14 December 2009)

We correlate the experimentally measured fracture toughness of 24 metals and ceramics to their quantum mechanically calculated brittleness parameter. The brittleness parameter is defined as the ratio of the elastic energy density needed to spontaneously break bonds in shear versus in tension, and is a primitive-cell property. Under 300 GPa hydrostatic pressure, the model predicts that diamond has smaller brittleness than molybdenum at zero pressure, and thus should deform plastically without cracking at room temperature. © *2009 American Institute of Physics*. [doi:10.1063/1.3267158]

I. INTRODUCTION

Fracture toughness K_{IC} measures the resistance of a material against crack propagation.[1] Metals are much tougher than ceramics, for example $K_{IC}(\text{silver})/K_{IC}(\text{silicon}) \sim 100$, despite their bulk modulus B are both near 100 GPa.[2] Thus, K_{IC} is not a function of *just* the scalar bonding energy. On the other hand, there are other fundamental mechanical and quantum mechanical attributes of bonding, such as the ideal strengths,[3–5] band gap,[6] ionicity,[7,8] etc., which one could correlate with K_{IC}. These intrinsic bonding attributes can all be obtained from *primitive-cell ab initio* calculations.[3–5,7,8] Undoubtedly, the microstructure of a material (heterogeneities and interfaces) can significantly influence its macroscopic K_{IC}. But here, we will demonstrate that bonding attributes at the primitive-cell level is still the most important factor.

II. THEORY

We follow the work of Rice and Thomson,[9] who proposed that a material is intrinsically brittle if

$$\frac{Gb}{\gamma_s} > 7.5 - 10, \tag{1}$$

where G is the shear modulus and b is the Burgers vector of the operative slip system, and γ_s is the surface energy of the cleavage plane. Later, Rice introduced the concept of unstable stacking energy γ_{us},[10] which is "the maximum energy encountered in the blocklike sliding along a slip plane, in the Burgers vector direction, of one half of a crystal relative to the other." The γ_{us} is a powerful parameter for analyzing dislocation nucleation energetics in front of an existing crack.[11]

The γ_{us} and γ_s are not primitive-cell properties. To calculate them requires more expensive slab setup[3] which usually contains more atoms than primitive-cell model. Also, to seek a simple measure of the brittleness of a crystal from first-principles calculations, we cannot use experimental information about operative slip systems and cleavage planes, but need to address the auxiliary questions also: what measures determine the likely slip systems and cleavage planes among the infinite crystallographic possibilities?

We propose that an alternative expression to Eq. (1), which can be defined at the primitive-cell level, is the dimensionless parameter

$$\beta \equiv \frac{w_{\text{shear}}}{w_{\text{decohesion}}}, \tag{2}$$

where w_{shear} and $w_{\text{decohesion}}$ are the minimum affine shear and tensile strain energy injected per primitive-cell volume (unit $\text{eV}/\text{Å}^3$) to induce spontaneous bond breaking at $T=0$ K. Furthermore, we hypothesize that the affine strain modes which minimize w_{shear} or $w_{\text{decohesion}}$ suggest the likely slip systems and cleavage planes.

In a previous work, we have analyzed 22 metals and ceramics using high-precision plane wave density functional theory (DFT) calculations.[12] The *ab initio* calculated equilibrium (zero-stress) lattice parameters and resolved elastic moduli are usually in very good agreement with experiments. For completeness, we list the calculation conditions in Table I, adding the data for TiC and TiN.

The w_{shear} is defined as

$$w_{\text{shear}} \equiv \min_{\text{shear mode}} \frac{E(\boldsymbol{\eta}_{\text{ideal}}) - E_0}{\Omega_0} = \min_{\text{shear mode}} \int_0^{\boldsymbol{\eta}_{\text{ideal}}} \frac{\Omega}{\Omega_0} \text{Tr}(\boldsymbol{\tau}\mathbf{J}^{-T} d\boldsymbol{\eta}\mathbf{J}^{-1}), \tag{3}$$

where Ω_0 and E_0 are the primitive-cell equilibrium volume and energy, respectively, $E(\boldsymbol{\eta}_{\text{ideal}})$ is the primitive-cell total energy at the point of affine shear-induced lattice instability, $\boldsymbol{\eta}$ is the Lagrangian strain tensor with respect to the equilibrium state, $\boldsymbol{\tau}$ is the Cauchy stress usually provided by the DFT program, and $\mathbf{J}$ is the affine transformation matrix relating the equilibrium and present states, with the present primitive-cell volume $\Omega/\Omega_0 = \det|\mathbf{J}|$. Derivation of the second equality can be found in Ref. 13, which is a large-strain formulation, but we need only the first equality to evaluate w_{shear} if we know the ideal shear strain $\boldsymbol{\eta}_{\text{ideal}}$. The relation

a)Electronic mail: liju@seas.upenn.edu.

TABLE I. *Ab initio* calculation conditions and equilibrium properties.

Material	# atoms	Method	# $\boldsymbol{k}$-points	E_{cut} [eV]	a_0, c_0 [Å] calc.	a_0, c_0 [Å] expt.	Expt. elastic const [GPa] C_{13}	C_{33}	C_{11}	C_{12}	C_{44}
Diamond	2	US-LDA	$6\times6\times6$	358.2	3.53	3.567[c]			1079.3	125	578.9[d]
Si	2	US-LDA	$5\times5\times5$	188.2	5.39	5.4238[d]			167	65	80[d]
β-SiC	2	US-LDA	$6\times6\times6$	358.2	4.32	4.36[d]			390	142	256[e]
α-Si_3N_4	28	US-LDA	$4\times4\times4$	434.8	7.70,5.58	7.818,5.591[f]	⋯	⋯	⋯	⋯	⋯
β-Si_3N_4	14	US-LDA	$4\times4\times8$	434.8	7.56,2.88	7.595,2.9023[g]	127	574	433	195	108[h]
TiC	8	US-LDA	$15\times15\times15$	358.2	4.27	4.317[i]			513	106	178[i]
TiN	8	US-LDA	$15\times15\times15$	434.8	4.18	4.240[i]			625	165	163[i]
NaCl	8	US-LDA	$6\times6\times6$	274.1	5.46	5.593[d]			57	11.5	13.3[d]
KBr	8	US-LDA	$6\times6\times6$	207.1	6.36	6.566[d]			43	4.8	5.4[d]
MgO	8	US-LDA	$6\times6\times6$	494.6	4.14	4.2072[d]			306	93	158[d]
CaO	8	US-LDA	$6\times6\times6$	494.6	4.57	4.80[d]			210	67	74[d]
Mo	1	US-GGA	$31\times31\times31$	233.1	3.15	3.1441[d]			476	158	111[d]
W	1	US-GGA	$31\times31\times31$	235.2	3.17	3.0213[d]			534	205	163[d]
Fe[a]	1	PAW-GGA	$31\times31\times31$	334.9	2.83	2.8603[j]			243	138	122[d]
Ti[b]	2	PAW-GGA	$27\times27\times17$	278.0	2.93,4.63	2.9457,4.6727[d]	68.3	190.5	176	86.9	50.8[k]
Mg	2	PAW-GGA	$39\times39\times25$	262.6	3.19,5.18	3.2094,5.2103[d]	21.7	66.5	63.5	25.9	18.4[d]
Zn	2	PAW-GGA	$33\times33\times23$	345.9	2.64,5.04	2.6638,4.9431[d]	52	69	178	35	46[d]
TiAl	4	US-GGA	$21\times21\times21$	226.5	3.98,4.08	3.975,4.068[l]	74.8	182	187	74.8	109[l]
Ti_3Al	8	US-GGA	$15\times15\times17$	226.5	5.74,4.65	5.814,4.649[m]	62.6	225.1	183.2	89.0	64.1[m]
Al	6	US-GGA	$18\times25\times11$	161.5	4.04	4.0321[d]			114	62	30.8[d]
Ni[a]	1	US-GGA	$31\times31\times31$	302	3.53	3.5136[d]			262	151	132[d]
Cu	6	US-GGA	$12\times17\times7$	292.2	3.64	3.616[d]			176.2	124.9	81.8[d]
Ag	1	US-LDA	$31\times31\times31$	225.8	4.02	4.07[d]			132	97	51[d]
Au	1	US-LDA	$43\times43\times43$	224.6	4.06	4.08[d]			202	169	45.3[d]

[a]Ferromagnetic.
[b]*p*-valence.
[c]Reference 23.
[d]Reference 24.
[e]Reference 25.
[f]Reference 26.
[g]Reference 27.
[h]Reference 28.
[i]Reference 29.
[j]Reference 30.
[k]Reference 31.
[l]Reference 32.
[m]Reference 33.

between ideal strain $\boldsymbol{\eta}_{\text{ideal}}$ and phonon instability is well studied[14–17] and not repeated here.

There are two modes to perform affine shear. One is *relaxed* shear, where $\boldsymbol{\tau}=\tau(\mathbf{b}\mathbf{n}^T+\mathbf{n}\mathbf{b}^T)$, $\mathbf{b}\perp\mathbf{n}$, $|\mathbf{b}|=|\mathbf{n}|=1$, and $\mathbf{J}$ are relaxed. The other is *unrelaxed* shear, where $\mathbf{J}=\mathbf{I}+g\mathbf{b}\mathbf{n}^T$ and g are parametrically varied, in which case $\Omega/\Omega_0=\det|\mathbf{J}|=1$, but stress components other than the resolved shear stress will generally be present. In this paper, we use w_{shear} values based on relaxed shear.

We have largely verified the hypothesis that the minimizers of w_{shear} predict the likely slip system. For instance, in fcc Al, Ni, Ag, Au, and Cu, $\{111\}\langle11\bar{2}\rangle$ affine shear has by far the lowest w_{shear} among all crystallographic possibilities, indicating correlated partial dislocation slip. In bcc Mo, W, and Fe, $\{110\}\langle\bar{1}11\rangle$, $\{211\}\langle\bar{1}11\rangle$, and $\{321\}\langle\bar{1}11\rangle$ affine shears have the lowest and almost degenerate w_{shear} values suggesting possible pencil glide.[18] In hcp metals, the minimizer of w_{shear} correctly predicts the preference of basal versus prism slip, with the exception of Ti. Such abnormality could be due to DFT error; but even when such slip system ranking error occurs, the difference in w_{shear} value is so small that it will not impact the Eq. (2) brittleness scale significantly.

In parallel to w_{shear}, $w_{\text{decohesion}}$ is defined as

$$w_{\text{decohesion}} \equiv \min_{\text{decohesion mode}} \frac{E(\boldsymbol{\eta}_{\text{ideal}})-E_0}{\Omega_0} = \min_{\text{decohesion mode}} \int_0^{\boldsymbol{\eta}_{\text{ideal}}} \frac{\Omega}{\Omega_0}\text{Tr}(\boldsymbol{\tau}\mathbf{J}^{-T}d\boldsymbol{\eta}\mathbf{J}^{-1}), \quad (4)$$

where $\boldsymbol{\eta}_{\text{ideal}}$ is the ideal tensile strain. Theoretically, uniaxial tension ($\boldsymbol{\tau}=\tau\mathbf{n}\mathbf{n}^T$) with Poisson relaxation might be physically the most relevant decohesion mode, because solids usually fracture by breaking bonds on an atomic plane only, instead of atomization. But, we have collected less *ab initio* calculation data in the relaxed uniaxial tension mode. It is practically much easier to generate *ab initio* calculation data in the unrelaxed hydrostatic tension mode: $\mathbf{J}=(\Omega/\Omega_0)^{1/3}\mathbf{I}$, in which scenario Eq. (4) is simplified to

TABLE II. Calculated shear modulus G_r (relaxed), bulk modulus B, ideal shear strain (relaxed) $\gamma_{\text{ideal}}^{\text{shear}}$ and ideal shear strength τ_{ideal}, ideal tensile strength σ_{ideal}, maximum strain energy density in shear w_{shear} and tension $w_{\text{decohesion}}$, and experimentally measured fracture toughness K_{IC}. Shear related value are always taken for common slip systems of materials. Fracture toughnesses K_{IC} are taken from Ref. 2 unless otherwise specified. $K_{\text{IC}}^{\text{max}}$ and $K_{\text{IC}}^{\text{min}}$ are upper and lower limit of fracture toughness of materials.

		[GPa]	[GPa]				[GPa]	[GPa]		[$\times 10^{-2}$ eV/A^3]			K_{IC}[MPa$\sqrt{\text{m}}$]	
Material	Slip system	G_r	B	B/G_r	(B/G_r) [a]	$\gamma_{\text{ideal}}^{\text{shear}}$	τ_{ideal}	σ_{ideal}	$\sigma_{\text{ideal}}/\tau_{\text{ideal}}$	w_{shear}	$w_{\text{decohesion}}$	β^{-1}	$K_{\text{IC}}^{\text{max}}$	$K_{\text{IC}}^{\text{min}}$
Diamond	$\{111\}\langle 110\rangle$	514.1	456.5	0.888	0.877	0.325	113.378	88.536	0.781	14.099	25.622	1.817	3.7	3
Si	$\{111\}\langle 110\rangle$	55.2	97.8	1.772	1.709	0.275	9.625	15.425	1.603	0.892	3.639	4.078	0.9	0.7
β-SiC	$\{111\}\langle 110\rangle$	158.2	236.3	1.494	1.502	0.350	31.738	40.587	1.279	4.585	10.701	2.333	5.1	2.3
α-Si_3N_4	$\{11\bar{2}0\}\langle 0001\rangle$	127.3	224.2	1.761	⋯	0.259	23.717	41.490	1.749	2.270	8.241	3.630	⋯	⋯
β-Si_3N_4	$\{10\bar{1}0\}\langle 0001\rangle$	101.0	242.0	2.396	2.398	0.232	19.000	45.974	2.420	1.521	12.057	7.926	10[d]	4.4
TiC	$\{110\}\langle 1\bar{1}0\rangle$	246.9	265.6	1.076	1.188	0.269	40.503	50.060	1.236	4.395	13.741	3.126	3	2
TiN	$\{110\}\langle 1\bar{1}0\rangle$	294.6	288.1	0.978	1.384	0.202	36.849	54.606	1.482	3.022	14.643	4.845	4.28	4.28[e]
NaCl	$\{110\}\langle 1\bar{1}0\rangle$	29.4	27.5	0.935	1.170	0.221	3.693	5.059	1.370	0.336	1.231	3.663	0.19	0.1
KBr	$\{110\}\langle 1\bar{1}0\rangle$	23.2	18.6	0.802	0.917	0.211	2.624	3.077	1.172	0.239	0.748	3.136	⋯	⋯
MgO	$\{110\}\langle 1\bar{1}0\rangle$	109.5	155.5	1.420	1.541	0.270	17.086	31.002	1.814	1.850	9.687	5.237	2.8	2.7
CaO	$\{110\}\langle 1\bar{1}0\rangle$	101.3	100.9	0.996	1.603	0.277	16.178	22.620	1.398	1.798	7.069	3.930	⋯	⋯
Mo	$\{110\}\langle \bar{1}11\rangle$	126.5	248.4	1.964	1.904	0.190	15.182	43.167	2.843	1.148	10.263	8.941	40	20
W	$\{110\}\langle \bar{1}11\rangle$	153.7	303.7	1.976	1.919	0.179	17.524	50.172	2.863	1.254	12.397	9.952	150	120
Fe[b]	$\{110\}\langle \bar{1}11\rangle$	76.6	213.4	2.785	2.667	0.178	8.140	28.448	3.495	0.590	7.611	12.890	150	120
Ti[c]	$\{1\bar{1}00\}\langle 11\bar{2}0\rangle$	47.6	116.8	2.454	2.463	0.099	2.822	21.483	7.613	0.114	6.065	53.010	55	50
Mg	$\{0001\}\langle 11\bar{2}0\rangle$	19.2	35.3	1.839	2.004	0.152	1.839	6.008	3.268	0.108	1.413	13.040	18	16
Zn	$\{0001\}\langle 11\bar{2}0\rangle$	36.6	82.3	2.249	1.412	0.132	2.116	9.542	4.510	0.117	1.602	13.733	115	60
TiAl	$\{111\}\langle 11\bar{2}\rangle$	50.0	107.5	2.150	1.908	0.218	5.543	19.842	3.580	0.481	5.150	10.698	8	8[f]
Ti_3Al	$\{1\bar{1}00\}\langle 11\bar{2}0\rangle$	50.0	117.2	2.344	2.404	0.127	5.505	20.783	3.775	0.247	4.680	18.956	18	14
Al	$\{111\}\langle 11\bar{2}\rangle$	25.4	72.4	2.850	2.899	0.200	2.840	11.148	3.925	0.225	1.452	6.444	35	30
Ni[b]	$\{111\}\langle 11\bar{2}\rangle$	60.1	199.8	3.324	2.732	0.140	5.050	29.244	5.791	0.301	6.812	22.590	150	100
Cu	$\{111\}\langle 11\bar{2}\rangle$	31.0	137.3	4.429	4.255	0.137	2.165	20.371	9.410	0.133	4.505	33.861	107	100
Ag	$\{111\}\langle 11\bar{2}\rangle$	25.0	107.0	4.280	4.854	0.145	1.647	17.621	10.699	0.120	4.350	36.357	105	70
Au	$\{111\}\langle 11\bar{2}\rangle$	17.9	181.2	10.120	8.621	0.105	0.850	23.448	27.572	0.041	4.315	104.287	90	60

[a]Computed analytically from expt. elastic constants of Table I.
[b]Ferromagnetic.
[c]p-valence.
[d]Reference 34.
[e]Reference 35.
[f]Reference 36.

$$w_{\text{decohesion}} = \frac{1}{3\Omega_0}\int_0^{\gamma_{\text{ideal}}} \text{Tr}(\boldsymbol{\tau})d\Omega. \tag{5}$$

In this paper, we use Eq. (5) to define the brittleness scale β expediently, while acknowledging that using uniaxial tensile $w_{\text{decohesion}}$ values will probably be physically more meaningful.

The purpose of defining β parameter is to contrast the strain energy cost of breaking a bond in shear versus breaking it in tension. If the former is very large, it will be kinetically easier to relax the stored elastic energy by cleavage. The problem with the cleavage mode of dissipation is that one quickly runs out bonds to break as sharp cracks run through and separate the material. On the other hand, if it takes less strain energy to break a bond in shear, it will be kinetically easier to activate the dislocation slip mode of dissipation. The key difference between breaking bonds in shear and in tension is geometric. After bonds are broken in shear, new bonds will generally form between new atomic neighbors, whereas if cleaved the atoms will be too far apart to form new bonds. So bonds are very much "renewable resources" in the shear mode of dissipation, but "nonrenewable" in cleavage mode of dissipation. Metals are tougher than ceramics because strain energy is continuously converted into heat as bonds break in shear, but then, reform and atoms slide past each other repeatedly in the crack-tip process zone.

Since the fracture toughness K_{IC} has unit MPa$\sqrt{\text{m}}$, to compare many different materials it is proper to scale it by

$$\tilde{K}_{\text{IC}} \equiv \frac{K_{\text{IC}}}{B(\Omega_0/N)^{1/6}}, \tag{6}$$

where N is the number of atoms per primitive-cell. $\tilde{K}_{\text{IC}}$ is then the dimensionless fracture toughness. Ceramics typically have $\tilde{K}_{\text{IC}}$ on the order of 1, while ductile metals usually have $\tilde{K}_{\text{IC}}$ on the order of a hundred (see Table II).

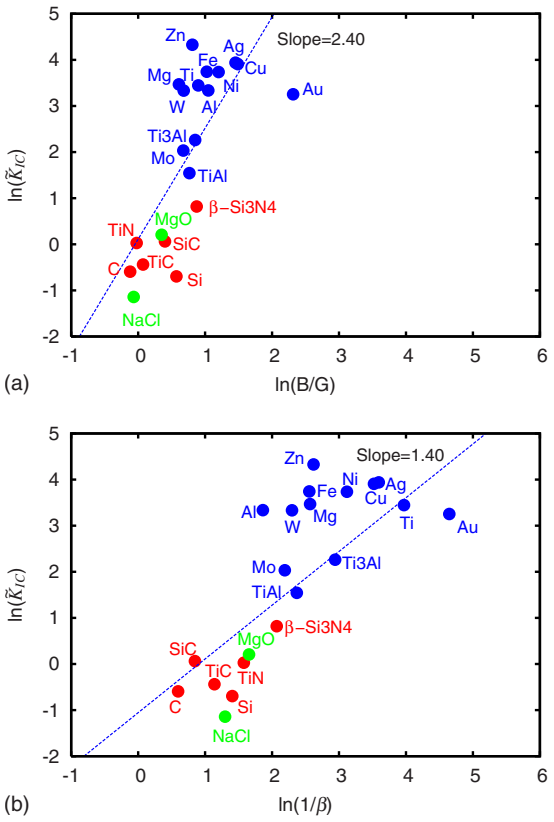

FIG. 1. (Color online) (a)Fracture toughness $\tilde{K}_{IC}$ vs B/G_r (metallic: blue, ionic: green, covalent: red). The mean value between K_{IC}^{max} and K_{IC}^{min} is used as representative fracture toughness of solids. The averaged fracture toughness is normalized as the Eq. (6) using value in Tables I and II. (b) Fracture toughness vs bond toughness β^{-1} of various crystalline solids (metallic: blue, ionic: green, covalent: red).

III. RESULTS AND DISCUSSION

Previously, the ratio of bulk modulus to shear modulus, B/G, has been used as an *ab initio* measure and predictor of ductility.[19] The correlation of $\ln(\tilde{K}_{IC})$ to $\ln(B/G)$ is plotted in Fig. 1(a). We can see that B/G indeed correlates with the experimental toughness $\tilde{K}_{IC}$, but variance of residuals (reduced chisquare) in $\ln(\tilde{K}_{IC})$, is large: 1.613, and correlation coefficient is small: 0.748. In contrast, the correlation of $\ln(\tilde{K}_{IC})-\ln(\beta^{-1})$ is shown in Fig. 1(b). The variance of residuals and the correlation coefficient are improved to 1.377 and 0.790, respectively. Furthermore, there is now an almost linear relationship (power-law exponent 1.4) between the experimentally measured fracture toughness $\tilde{K}_{IC}$ and the *ab initio* calculated β^{-1}, which also range from order 1 for ceramics to order 10^2 for ductile metals (see Table II).

The superiority of β parameter to B/G might be expected, because B and G characterize the linear response of the crystal to small bond distortions. But to activate the dissipation modes, the bonds need to be distorted to the extremes and eventually broken. The β parameter describes such nonlinear physics. w_{shear} and $w_{decohesion}$ are related to B and G, but contain extra information about the "stretchability" and "shearability" of bonds.[12] Thus, if a single lumped parameter is desired to rank the intrinsic brittleness of a material, β could be the more physically reasonable parameter at the primitive-cell level. Since β describes the intrinsic or bond brittleness, it might be consistent to call $\beta^{-1}=w_{decohesion}/w_{shear}$ the intrinsic toughness or bond toughness.

When biased by an external stress τ_{ext}, such as a confining hydrostatic pressure, β can be shifted

$$\beta(\boldsymbol{\tau}_{ext}) \equiv \frac{w_{shear}(\boldsymbol{\tau}_{ext})}{w_{decohesion}(\boldsymbol{\tau}_{ext})}, \tag{7}$$

where

$$w_{shear}(\boldsymbol{\tau}_{ext}) = \min_{shear\ mode} \int_0^{\boldsymbol{\eta}_{ideal}(\boldsymbol{\tau}_{ext})} \frac{\Omega}{\Omega_0(\boldsymbol{\tau}_{ext})} \times \mathrm{Tr}[(\boldsymbol{\tau}+\boldsymbol{\tau}_{ext})\mathbf{J}^{-T} d\boldsymbol{\eta}\mathbf{J}^{-1}], \tag{8}$$

and

$$w_{decohesion}(\boldsymbol{\tau}_{ext}) = \min_{decohesion\ mode} \int_0^{\boldsymbol{\eta}_{ideal}(\boldsymbol{\tau}_{ext})} \frac{\Omega}{\Omega_0(\boldsymbol{\tau}_{ext})} \times \mathrm{Tr}[(\boldsymbol{\tau}+\boldsymbol{\tau}_{ext})\mathbf{J}^{-T} d\boldsymbol{\eta}\mathbf{J}^{-1}]. \tag{9}$$

Figures 2(a) and 2(b) show $w_{decohesion}$ and w_{shear} for crystalline diamond under 0, 100, 200, and 300 GPa external hydrostatic pressure. $w_{decohesion}$ increases substantially with increasing external pressure, whereas w_{shear} does not show significant change. As a result, the bond toughness increases with pressure, as shown in Fig. 2(c). Hence, at 300 GPa pressure, the dimensionless toughness level of diamond matches that of BCC Mo of zero pressure. Then, diamond may exhibit ductile response at room-temperature like metals, although it is quite brittle at zero pressure.

Here, it should be noted that in a precise sense the shaded regions in Fig. 2(a) are not equal to w_{shear} because of the nonzero volumetric strain during shearing. The volumetric strain in the shearing process, less than 0.002 for diamond, is however much smaller than $\boldsymbol{\eta}_{ideal}$. Therefore, Fig. 2(a) gives a good estimate of w_{shear}. β in Fig. 2(c) are exactly computed using Eq. (7) which automatically includes volume change.

Many high-pressure experiments using diamond anvil and indenter have been performed recently.[20,21] In these experiments, we can observe dislocation activities in diamond crystal even at room temperature. One expects high pressures of 10%–30% of bulk modulus beneath the indenter,[22] and therefore diamond chooses the shear energy-dissipation mode rather than the cleavage mode in such condition. This fact could support our discussion above.

IV. CONCLUSIONS

We define a simple measure of brittleness and then evaluate it for 24 metals and ceramics using first-principles calculations. We confirm that the brittleness is reasonably correlated with the experimental fracture toughness K_{IC}. The brittleness defined this way naturally depends on external hydrostatic pressure. As a result, we predict that diamond has the ability to deform plastically like metals at room temperature if under more than 250 GPa hydrostatic pressure.

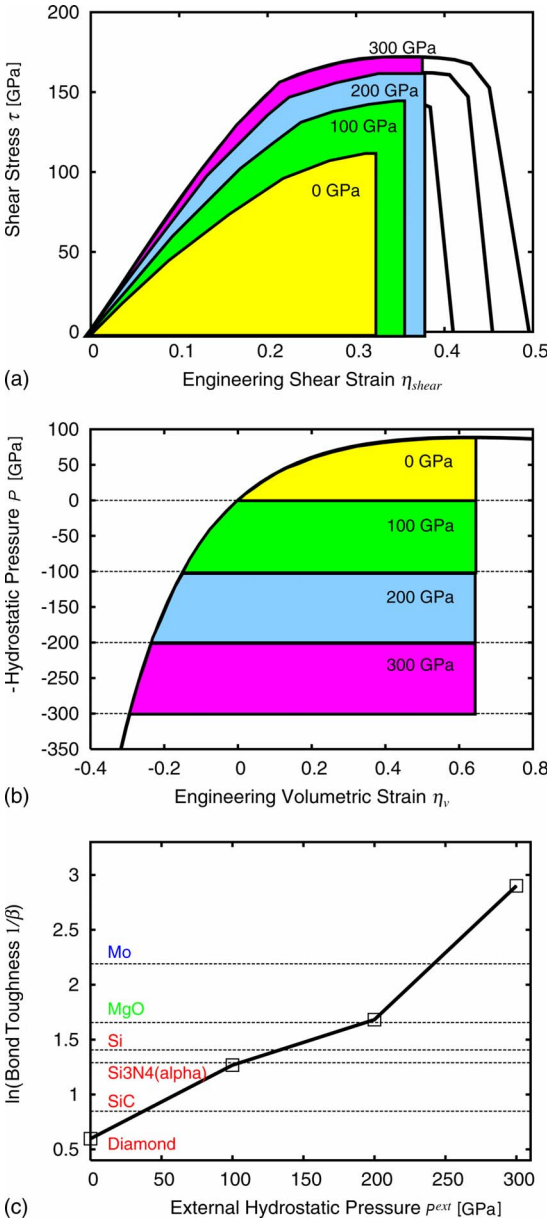

FIG. 2. (Color online) (a) Shear stress-strain relation of diamond crystal for the slip system {111}⟨110⟩ under hydrostatic pressure 0, 100, 200, and 300 GPa, respectively. Work needed to realize irreversible shear deformation under each hydrostatic pressure can be estimated by the colored area plus work against the external hydrostatic pressure due to volume change. (b) Hydrostatic pressure-volumetric strain curve of diamond crystal. Work needed to break bonds at each hydrostatic pressure can be estimated by the colored area. (c) Bond toughness parameter of diamond as a function of hydrostatic pressure. The bond toughness goes up to metallic level at the hydrostatic pressure of 250 GPa.

ACKNOWLEDGMENTS

S.O. acknowledges support by the Ministry of Education, Culture, Sports, Science and Technologies in Japan, Grant-in-Aid for Scientific Research B (Grant No. 20360055) and support by Grand Challenges in Next-Generation Integrated Nanoscience Project. J.L. acknowledges support by NSF (Grant No. CMMI-0728069), ONR (Grant No. N00014-05-1-0504), AFOSR (Grant No. FA9550-08-1-0325), and Ohio Supercomputer Center.

[1]M. F. Ashby, *Materials Selection in Mechanical Design*, 3rd ed. (Elsevier, Amsterdam, 2005).
[2]M. F. Ashby and D. Cebon, *Cambridge Engineering Selector (CES)* (Granta Design Limited, Cambridge, 2006).
[3]S. Ogata, J. Li, and S. Yip, Science **298**, 807 (2002).
[4]J. W. Morris, D. M. Clatterbuck, D. C. Chrzan, C. R. Krenn, W. Luo, and M. L. Cohen, Mater. Sci. Forum **426–432**, 4429 (2003).
[5]J. Pokluda, M. Černý, P. Sandera, and M. Šob, J. Comput. Aided Mater. Des. **11**, 1 (2004).
[6]J. J. Gilman, *Electronic Basis of the Strength of Materials* (Cambridge University Press, Cambridge, 2003).
[7]F. M. Gao, J. L. He, E. D. Wu, S. M. Liu, D. L. Yu, D. C. Li, S. Y. Zhang, and Y. J. Tian, Phys. Rev. Lett. **91**, 015502 (2003).
[8]A. Simunek and J. Vackar, Phys. Rev. Lett. **96**, 085501 (2006).
[9]J. R. Rice and R. Thomson, Philos. Mag. **29**, 73 (1974).
[10]J. R. Rice, J. Mech. Phys. Solids **40**, 239 (1992).
[11]J. Li, MRS Bull. **32**, 151 (2007).
[12]S. Ogata, J. Li, N. Hirosaki, Y. Shibutani, and S. Yip, Phys. Rev. B **70**, 104104 (2004).
[13]J. H. Wang, J. Li, S. Yip, S. Phillpot, and D. Wolf, Phys. Rev. B **52**, 12627 (1995).
[14]J. Li and S. Yip, Comput. Model. Eng. Sci. **3**, 219 (2002).
[15]D. M. Clatterbuck, C. R. Krenn, M. L. Cohen, and J. W. Morris, Phys. Rev. Lett. **91**, 135501 (2003).
[16]S. V. Dmitriev, T. Kitamura, J. Li, Y. Umeno, K. Yashiro, and N. Yoshikawa, Acta Mater. **53**, 1215 (2005).
[17]F. Liu, P. M. Ming, and J. Li, Phys. Rev. B **76**, 064120 (2007).
[18]D. Roundy, C. R. Krenn, M. L. Cohen, and J. W. Morris, Philos. Mag. A **81**, 1725 (2001).
[19]L. Vitos, P. A. Korzhavyi, and B. Johansson, Nature Mater. **2**, 25 (2003).
[20]H. Sumiya, K. Yamaguchi, and S. Ogata, Appl. Phys. Lett. **88**, 161904 (2006).
[21]Y. Nakamoto, H. Sumiya, T. Matsuoka, K. Shimizu, T. Irifune, and Y. Ohishi, Jpn. J. Appl. Phys. **46**, L640 (2007).
[22]T. Zhu, J. Li, K. J. Van Vliet, S. Ogata, S. Yip, and S. Suresh, J. Mech. Phys. Solids **52**, 691 (2004).
[23]J. Donohue, *The Structures of the Elements*, 2nd ed. (Wiley, New York, 1974).
[24]H. Landolt, R. Börnstein, and K. H. Hellwege, *Landolt-Börnstein* (Springer-Verlag, Berlin, 1973).
[25]W. R. L. Lambrecht, B. Segall, M. Methfessel, and M. Vanschilfgaarde, Phys. Rev. B **44**, 3685 (1991).
[26]K. Kato, Z. Inoue, K. Kijima, I. Kawada, H. Tanaka, and T. Yamane, J. Am. Ceram. Soc. **58**, 90 (1975).
[27]R. Grün, Acta Crystallogr., Sect. B: Struct. Crystallogr. Cryst. Chem. **35**, 800 (1979).
[28]R. Vogelgesang, M. Grimsditch, and J. S. Wallace, Appl. Phys. Lett. **76**, 982 (2000).
[29]R. Ahuja, O. Eriksson, J. M. Wills, and B. Johansson, Phys. Rev. B **53**, 3072 (1996).
[30]M. Acet, H. Zähres, E. F. Wassermann, and W. Pepperhoff, Phys. Rev. B **49**, 6012 (1994).
[31]E. S. Fisher and C. J. Renken, Phys. Rev. **135**, A482 (1964).
[32]K. Tanaka, T. Ichitsubo, H. Inui, M. Yamaguchi, and M. Koiwa, Philos. Mag. Lett. **73**, 71 (1996).
[33]K. Tanaka, K. Okamoto, H. Inui, Y. Minonishi, M. Yamaguchi, and M. Koiwa, Philos. Mag. A **73**, 1475 (1996).
[34]F. L. Riley, J. Am. Ceram. Soc. **83**, 245 (2000).
[35]H. Kuwahara, N. Mazaki, M. Takahashi, T. Watanabe, X. Yang, and T. Aizawa, Mater. Sci. Eng., A **319**, 687 (2001).
[36]K. T. V. Rao, G. R. Odette, and R. O. Ritchie, Acta Metall. Mater. **40**, 353 (1992).